Oxidation of guaiacol by myeloperoxidase: a two-electron-oxidized guaiacol transient species as a mediator of NADPH oxidation

Chantal CAPEILLÈRE-BLANDIN[1]

Laboratoire de chimie et biochimie pharmacologiques et toxicologiques, CNRS URA 400, Université René Descartes, Paris V, 45 rue des Saints Pères, 75270 Paris Cedex 06, France

The present study was first aimed at a complete steady-state kinetic analysis of the reaction between guaiacol (2-methoxyphenol) and the myeloperoxidase (MPO)/H_2O_2 system, including a description of the isolation and purification of MPO from human polymorphonuclear neutrophil cells. Secondly, the overall reaction of the oxidation of NADPH, mediated by the reactive intermediates formed from the oxidation of guaiacol in the MPO/H_2O_2 system, was analysed kinetically. The presence of guaiacol stimulates the oxidation of NADPH by the MPO/H_2O_2 system in a concentration-dependent manner. Concomitantly, the accumulation of biphenoquinone (BQ), the final steady-state product of guaiacol oxidation, is lowered, and even inhibited completely, at high concentrations of NADPH. Under these conditions, the stoichiometry of NADPH:H_2O_2 is 1, and the oxidation rate of NADPH approximates to that of the rate of guaiacol oxidation by MPO. The effects of the presence of superoxide dismutase, catalase and of anaerobic conditions on the overall oxidation of NADPH have also been examined, and the data indicated that superoxide formation did not occur. The final product of NADPH oxidation was shown to be enzymically active $NADP^+$, while guaiacol was generated continuously from the reaction between NADPH and oxidized guaiacol product. In contrast, similar experiments performed on the indirect, tyrosine-mediated oxidation of NADPH by MPO showed that a propagation of the free radical chain was occurring, with generation of both $O_2^{-\bullet}$ and H_2O_2. BQ, in itself, was able to spontaneously oxidize NADPH, but neither the rate nor the stoichiometry of the reaction could account for the NADPH-oxidation process involved in the steady-state peroxidation cycle. These results provide evidence that the oxidation of NADPH does not involve a free nucleotide radical intermediate, but that this is probably due to a direct electron-transfer reaction between NADPH and a two-electron-oxidized guaiacol intermediate.

INTRODUCTION

Phagocytosis by polymorphonuclear leukocytes results in the formation of a series of reactive oxygen metabolites during a respiratory burst of non-mitochondrial O_2 uptake [1]. Simultaneously, an increase in glucose oxidation via the hexose monophosphate shunt, and a decrease in the NADPH/$NADP^+$ ratio, is observed [2]. Indeed, $NADP^+$ concentration becomes the rate-limiting factor for the dehydrogenases of the hexose monophosphate shunt [3].

Two key enzyme systems are involved in the oxidative stress reaction of phagocytes, producing oxygen derivatives. First is the NADPH oxidase, a membrane multienzyme complex, which catalyses the univalent reduction of molecular oxygen by NADPH and generates $O_2^{-\bullet}$ [4]. Subsequently, H_2O_2, which is also generated during the respiratory burst, is utilized by myeloperoxidase (MPO), an enzyme located in azurophil granules, which, in the presence of a suitable halide ion such as Cl^-, produces HOCl and related oxidative compounds, such as chloramines [5,6]. As found for other peroxidases, MPO can also catalyse the oxidation by H_2O_2 of a number of organic compounds, including phenolic compounds [7].

Mechanistic studies *in vitro* on peroxidases have been carried out extensively with phenolic compounds. The primary reaction products are considered to be phenoxyl radicals (G-O$^\bullet$), which are deactivated by non-enzymic transformations [8]. Guaiacol, the 2-*o*-methoxyphenol, has been frequently used as the hydrogen donor in the assaying of peroxidases [9,10]. During the course of the normal peroxidation cycle, the characteristic red–brown species developed from the oxidation of guaiacol by peroxidase was ascribed to guaiacol dimers with quinone residues [11], thus supporting the hypothetical rapid dimerization step involving cross-linking of phenoxyl radicals [12,13]. These results apparently contradicted the idea prevalent that tetraguaiacol formation was being monitored at 470 nm [14]. The true identity of the major steady-state peroxidase oxidation product of guaiacol was confirmed by the use of on-line HPLC and MS to be 3,3′-dimethoxy-4,4′-biphenylquinone [15], which is generated from the consumption of two H_2O_2 molecules, i.e. one H_2O_2 per molecule of guaiacol.

The catalytic cycle of MPO is similar to most peroxidases that perform one-electron oxidation of organic substrates to radicals in two sequential one-electron steps via two intermediate forms of the enzyme, compounds I and II. These are representative of states that are more oxidized than the native ferric form by either two or one electron(s) respectively. The mechanistic cycle that is, in general, widely accepted is as follows:

$$\text{Peroxidase} + H_2O_2 \rightarrow \text{CI} \quad (1)$$

$$\text{CI} + \text{G-OH} \rightarrow \text{CII} + \text{G-O}^\bullet \quad (2)$$

$$\text{CII} + \text{G-OH} \rightarrow \text{peroxidase} + \text{G-O}^\bullet \quad (3)$$

$$2\text{G-O}^\bullet + 2H^+ \rightarrow \text{HO-G-G-OH} \quad (4)$$

$$2\text{G-O}^\bullet \rightarrow \text{G-O}^- + \text{G-O}^+ \quad (5)$$

where G-OH is the phenolic substrate being oxidized [16] and CI and CII represent compounds I and II respectively. The fate of

Abbreviations used: BQ, biphenoquinone; HRP, horseradish peroxidase; LPO, lactoperoxidase; MPO, myeloperoxidase; SOD, superoxide dismutase; TPO, thyroid peroxidase.

[1] e-mail: blandin@bisance.citi2.fr

the phenoxyl radicals, generated in the first step [eqns. (1)–(3)], was described as a dimerization [8] [eqn. (4)]. The biphenol was subsequently found to undergo further oxidation to biphenoquinone (BQ) more readily than guaiacol [11].

A two-electron oxidation mechanism could be feasible if the phenoxyl radicals, G-O$^{\bullet}$, are deactivated by dismutation, leading to a phenoxyl cation [G-O^{+}; eqn. (5)], or if the catalytic cycle is completed by the one-electron reduction of compound II by phenoxyl radical:

$$\text{CII} + \text{G-O}^{\bullet} \rightarrow \text{peroxidase} + \text{G-O}^{+} \quad (3')$$

This electrophilic two-electron oxidation product (G-O^{+}) can undergo further polymerization to a more stable BQ, or a reaction with nucleophils. Depending on the reaction sequence followed, guaiacol could be considered as either a two- or a one-electron donor. However, previous reports [17] on phenol oxidation by peroxidases showed that the mechanism of oxidation of guaiacol catalysed by thyroid peroxidase (TPO) appeared to be a two-electron type, whereas the mechanism was invariably a one-electron type with horseradish peroxidase (HRP) or lactoperoxidase (LPO).

The major objectives of this study were to examine further the oxidation of guaicol by MPO and to investigate the mechanism of reaction, taking into account the importance of new kinetic data. The intermediates generated by peroxidases, free radicals and/or two-electron-oxidized products from phenols, are usually electrophilic and potent oxidants capable of participating in a variety of secondary non-enzymic redox reactions, involving a wide range of organic compounds, including NAD(P)H [8,18–20]. To shed light on the occurrence of these transient products formed from oxidation of guaiacol in the presence of MPO/H_2O_2, we studied both their reactivity and that of the final oxidation product, the BQ, in co-oxidation reactions involving NADPH. We characterized the reaction and present evidence here that NADPH oxidation does not involve radical chain reactions, as it does when tyrosine is assayed as a mediator, but involves a direct two-electron transfer mechanism to a transient oxidized gaiacol product. Part of these experiments were included in a preliminary report given at the Eurobic II 1994 meeting [21].

MATERIALS AND METHODS

Materials

Superoxide dismutase (SOD) from bovine erythrocytes, catalase from bovine liver and glucose-6-phosphate dehydrogenase from Baker's yeast were purchased from Sigma Chemical Co. (St Louis, MO, U.S.A.). Guaiacol, tetranitromethane, tyrosine and NADPH tetrasodium salt were also obtained from Sigma. All other chemicals used were of the highest grade available and prepared daily in distilled deionized water.

Purification of MPO

Human MPO isolated from polymorphonuclear leukocytes was extracted as a by-product of cytochrome b_{558} purification [22]. The MPO activity was extracted repeatedly from thawed cell pellets in a 1 % (v/v) cholate-lysing medium, and kept frozen at −80 °C. This extract was enriched by two successive $(NH_4)_2SO_4$ precipitations. The precipitate from the 45–65 % cut was dissolved in 0.1 M potassium phosphate buffer, pH 7.5, in the presence of 1 mM PMSF, before dialysing extensively against the same buffer and application to a heparin–agarose column (Sigma Type II) equilibrated with the same buffer. The adsorbed MPO was eluted at a flow rate of 35 ml/h with a 2 × 30 ml phosphate gradient, increasing from 0.1 to 0.5 M at pH 7.5. In contrast with published procedures based on cation-exchange chromatography [23,24], the haemoprotein (with MPO activity) was found to be eluted as a single symmetrical peak at a buffer concentration of 0.31 ± 0.01 M ($n = 5$). The eluate was then transferred by ultrafiltration to 20 mM Tris/HCl buffer (pH 8.6) in order to concentrate the enzyme present in fractions with a purity index (A_{430}/A_{280}) higher than 0.5. Further purification was performed by anion-exchange chromatography using a DEAE-Sepharose fast-flow column. The MPO was excluded and found in the wash fractions. The unadsorbed fractions were pooled, concentrated and stored at −80 °C. Alternatively, the latter chromatographic step could be replaced by the use of gel-filtration chromatography with a Superdex 200 gel (HiLoad 16/60 Superdex 200 prep. grade column from Pharmacia). In this case, the elution volume corresponded to a molecular mass of 150 kDa. The enzyme preparation used in this study exhibited a purity index from 0.74 to 0.83. All purification steps were performed at 4 °C.

Spectral measurements

Absorbance spectra, repetitive scans and kinetic absorbance measurements were performed using a Kontron Uvicon 942 interfaced with a computer to facilitate the collection, manipulation and analysis of data with the appropriate software.

Substrate and product concentration measurements

Hydrogen peroxide solutions were prepared by appropriate dilutions of 30 % (v/v) H_2O_2 (Sigma) in water distilled/deionized three times, of conductivity 1.3 μS. Their concentrations were determined by monitoring A_{240} using $\epsilon_{240} = 43.6\ \text{M}^{-1}\cdot\text{cm}^{-1}$ [25], and dilutions required were prepared daily.

The formation of oxidized product from guaiacol was followed, by spectrophotometric means, as the absorbance changes at 470 nm. The molar absorption coefficient was determined from the slope of linear plots of the maximum absorbance increase versus the number of hydrogen peroxide molecules consumed in MPO-catalysed reactions, where hydrogen peroxide was the limiting reagent (25–200 μM), assuming a total and equimolar reaction. A similar procedure had been followed previously [26] in the analysis of kinetic data for peroxidase-catalysed oxidation of phenols. Under steady-state conditions, this procedure reflects the amount of H_2O_2 consumed by the peroxidation reaction of one guaiacol molecule leading to one oxidized guaiacol product, or half a molecule of BQ. At pH 7.0, a value of $5.58 \pm 0.08\ \text{mM}^{-1}\cdot\text{cm}^{-1}$ ($n = 12$) was determined (see Figure 2, upper panel), close to the value of 5.53 reported with H_2O_2 and HRP enzyme [27].

MPO characteristics

The MPO concentration, expressed as haem concentration, was determined spectrophotometrically on the basis of Soret absorbance at 430 nm using a millimolar absorption coefficient per haem of $89\ \text{mM}^{-1}\cdot\text{cm}^{-1}$ [28]. In routine assays, the standard molar activity of MPO was defined under typical reaction conditions, consisting of a saturating concentration of 300 μM H_2O_2, 13.4 mM guaiacol and 20 nM MPO in 20 mM phosphate buffer, pH 7.0; this corresponded to $400 \pm 30\ \text{s}^{-1}$ ($n = 8$) at 20 °C for enzyme with a purity index $\geqslant 0.7$.

Steady-state kinetics of guaiacol oxidation

The mixture contained varying concentrations of guaiacol and H_2O_2 with 20–40 nM MPO (as specified in the legends of the Figures) in 20 mM phosphate buffer, pH 7.0. Reactions were

performed at 20 °C and initiated by addition of MPO. The rate of formation of the guaiacol oxidation product was determined from the increase in the A_{470} during the first 20 s, using a millimolar absorbance coefficient of 5.58 $mM^{-1} \cdot cm^{-1}$. For each concentration, measurements were made in duplicate. All experiments were repeated at least three times using different MPO preparations. The steady-state kinetic constants, k_{cat} and K_m, were determined by direct fit of the non-inhibited part of the plot to the Michaelis–Menten equation using a non-linear regression analysis program (Kaleidagraph).

Reaction of NADPH with guaiacol, MPO and H_2O_2

Stock solutions of NADPH were made daily in thrice-distilled, slightly alkaline water, defined by a conductivity measurement of 1.3 μS. Although NADPH absorbed maximally at 340 nm, in the presence of guaiacol, rates could not be accurately measured at this wavelength because the oxidation product of guaiacol also absorbed significantly. Therefore the oxidation of NADPH was studied at 330 nm, where the minimal absorbance level for guaiacol oxidation product was observed. The experimentally determined millimolar absorption coefficient of NADPH at 330 nm is 5.78 $mM^{-1} \cdot cm^{-1}$, whereas it is 1.2 $mM^{-1} \cdot cm^{-1}$ for oxidized guaiacol product. A cuvette with a 0.4-cm optical path was used for NADPH concentrations higher than 300 μM. Initial rates were determined by varying the concentrations of H_2O_2, guaiacol and NADPH in the presence of 20–30 nM MPO in 20 mM phosphate buffer, pH 7.0, at 20 °C. Kinetic constants were determined from the data for a minimum of three independent experiments. In parallel experiments, the reaction was followed at the level of guaiacol oxidation by monitoring A_{470}.

Reaction of NADPH with guaiacol BQ

Solutions of oxidized guaiacol were prepared using 30 nM MPO, 100 μM H_2O_2 and 1 mM guaiacol. The reaction was allowed to proceed to completion, corresponding to the maximal absorbance increase followed at 470 nm. At that time (generally 1–1.1 min), 5 μl of a concentrated solution of NADPH was added to ensure pseudo-first-order conditions. It caused an immediate exponential decrease in absorbance, owing to reduction of BQ, fitted to one exponential term by a non-linear iterative regression program (Kaleidagraph). Concomitant spectrophotometric measurements at 330 nm allowed monitoring of NADPH oxidation.

Redox cycles of guaiacol

The oxidation of NADPH and guaiacol was monitored by repetitive scans performed every minute between 600–300 nm in the presence of MPO (0.15 μM), and after repetitive addition of aliquots of H_2O_2 (90 μM) performed approx. every 3–4 min, up to the final extent of the reaction.

RESULTS

Steady-state kinetics of guaiacol oxidation by MPO

Time course of guaiacol oxidation

Figure 1 (upper panel, curve a) shows the kinetics of the oxidation of guaiacol by MPO + H_2O_2 to the appropriate BQ monitored at A_{470}. Under steady-state conditions, two kinetic phases with very different rates were observed. The initial formation was fairly linear with time over the first 40 s, reaching a maximal level at a rate of 43 s^{-1}, followed by a slow, distinct decline at a rate of 2×10^{-4} s^{-1}.

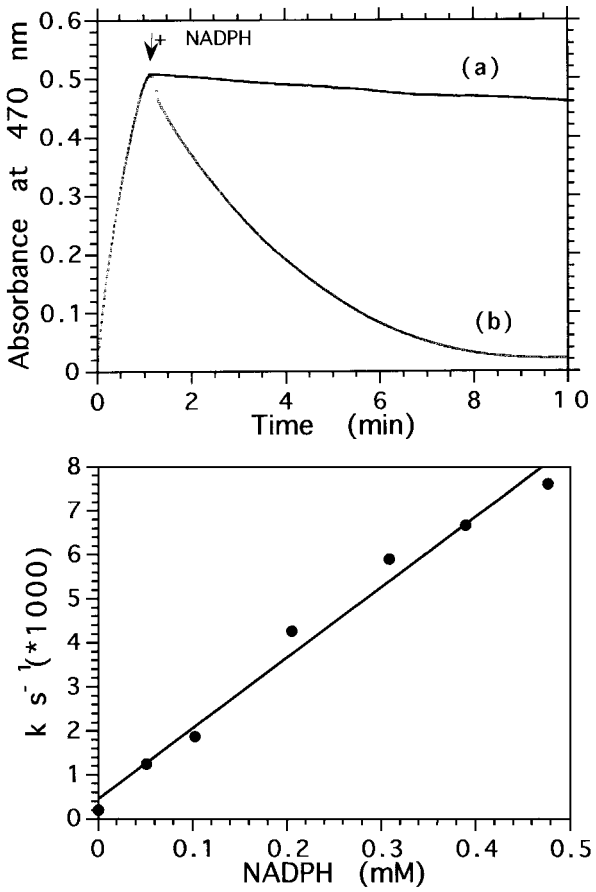

Figure 1 Time course of guaiacol oxidation

Upper panel: the kinetics of formation of BQ were monitored at 470 nm (line a). The reaction was initiated by addition of 34 nM MPO, expressed as the molar concentration of haem. When the full extent of guaiacol oxidation was attained (at 1.1 min), which corresponded to 91 μM of oxidized guaiacol, 300 μM NADPH was added and the exponential decay corresponded to $k = 6 \times 10^{-3}$ s^{-1} (line b), instead of 0.2×10^{-3} s^{-1} (line a). The reaction mixtures contained 20 mM phosphate buffer, pH 7.0, 1 mM guaiacol and 100 μM H_2O_2. In the lower panel is shown a second-order plot for the dependence of the decay rate on NADPH concentration; $k_+ = 16$ $M^{-1} \cdot s^{-1}$ ($r^2 = 0.98$).

The first phase was MPO-dependent, and corresponded to a high-rate step, which was further increased by addition of H_2O_2 and guaiacol. In the low-rate time course, the decay rate was not modified by further addition of MPO or 1 μM SOD, but the disappearance was accelerated by an increase in the concentration of free guaiacol, and became essentially instantaneous with the addition of a reductant, such as 1 mM ascorbic acid, glutathione or NADPH [Figure 1 (curve b) and below]. These observations confirmed that the BQ accumulated in the peroxidase-catalysed oxidation of guaiacol was a highly reactive oxidant, and that it was easily reduced, probably to biphenol, by either extraneous or endogenous reductants.

Variation in the extent of the reaction versus H_2O_2 concentration indicated that the ratio of the peak amount of guaiacol oxidized to the amount of H_2O_2 added is equal to 1 at saturating guaiacol concentrations, and for H_2O_2 concentrations below 250 μM (Figure 2, upper panel). In contrast, at a given H_2O_2 concentration of 100 μM, the extent of guaiacol oxidation increased with increasing concentrations of guaiacol, and the absorbance reached a plateau for guaiacol concentrations equal to or higher than 2 mM, thus also allowing an estimate to be

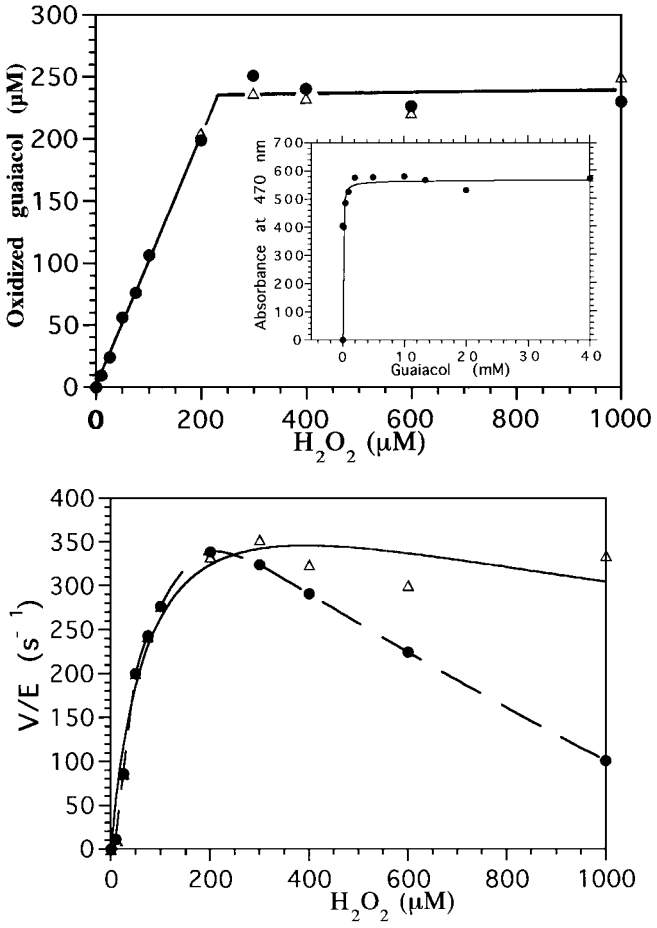

Figure 2 Effect of H_2O_2 concentration on the extent and rate of guaiacol oxidation

Upper panel: effect of H_2O_2 on the maximal recorded yield of oxidized guaiacol formation. The linear portion from 0 to 200 μM H_2O_2 allowed the determination of the molar absorbance coefficient of the guaiacol oxidation product, assuming a total and equimolar reaction, of $\Delta\epsilon = 5.58 \pm 0.08$ $mM^{-1} \cdot cm^{-1}$ ($n = 12$). The insert shows the effect of guaiacol on the maximal recorded yield of oxidized guaiacol obtained in the presence of 26 nM MPO and 100 μM H_2O_2. Here, the value of $\Delta\epsilon$ determined corresponded to 5.6 ± 0.1 $mM^{-1} \cdot cm^{-1}$. Lower panel: effect of H_2O_2 on the initial rate of formation of oxidized guaiacol, *V*/*E*, expressed as molar concentration of guaiacol oxidation product produced/s per molar concentration of MPO of haem. In both the upper and lower panels, reaction mixtures contained 16 nM MPO, 13.4 mM guaiacol and varying concentrations of H_2O_2 in 20 mM phosphate buffer, pH 7.0. The reaction was also performed in the presence of 20 μM tetranitromethane (△) added to certain incubations.

made for the molar absorption coefficient of one oxidized guaiacol molecule, as shown in the insert to Figure 2 (upper).

Effect of H_2O_2 concentration

Variation in the initial rate of oxidation of guaiacol as a function of H_2O_2 concentration is presented in Figure 2 (lower panel). The rate of formation of guaiacol oxidation product increased as the H_2O_2 concentrations increased up to the 200–300 μM range. A further increase in the H_2O_2 concentration resulted in a relatively constant yield of oxidation product, as determined by monitoring the maximal absorbance level recorded at 470 nm (Figure 2, upper), associated with a decrease in the rate of guaiacol oxidation. These data confirm that H_2O_2 inhibits MPO at high concentrations, as reported previously [5,7].

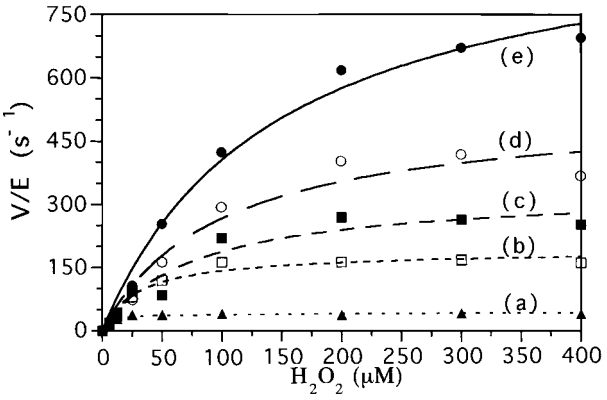

Figure 3 Steady-state kinetics for the oxidation of guaiacol by MPO

Dependence of the initial rate of formation of oxidized guaiacol, *V*/*E*, expressed in μM of oxidized guaiacol product/ μM of haem monomer per s on H_2O_2, and guaiacol concentrations. The lines through the data points were obtained by fitting the data to the Michaelis–Menten equation. Reaction mixtures contained 25 nM MPO, in 20 mM phosphate buffer, pH 7.0. The illustrated guaiacol concentrations, with curves represented by letters in parentheses, were (from bottom to top): (a), 1 mM; (b), 5 mM; (c), 10 mM; (d), 15 mM; (e), 35 mM.

SOD and tetranitromethane effects

In order to investigate the possible accumulation of MPO in an inactive form, i.e. compound III (Fe^{3+}–$O_2^{\cdot-}$), we added superoxide scavengers to the reaction mixture [29,30]. These scavengers had no effect on either the rate of formation or yield of oxidation product for H_2O_2 concentrations below 250 μM. However, at higher H_2O_2 concentrations (i.e. > 300 μM), the observed decrease in the rate of guaiacol oxidation was prevented by addition of 1 μM SOD or 20 μM tetranitromethane (Figure 2, lower panel). This observation is consistent with the accumulation of compound III, a catalytically inactive enzyme formed during the steady-state oxidation of guaiacol, thus accounting for the decreased rate at high H_2O_2 concentrations. It is noteworthy that this addition did not modify the yield of BQ formation (Figure 2, upper).

Steady-state parameters

Steady-state analyses as a function of H_2O_2 and different guaiacol concentrations yielded a family of curves, as illustrated in Figure 3. The maximal rate was obtained for 50 μM H_2O_2 at 0.2 mM guaiacol and shifted to 600 μM at 35 mM guaiacol. Under conditions of non-inhibiting H_2O_2 concentration, hyperbolic saturation curves were obtained for the variations of the initial rate of formation of oxidized guaiacol as a function of H_2O_2 concentration. Apparent k_{cat} and K_m values could be deduced by non-linear least-squares fitting, as illustrated in Table 1. k_{cat} values were dependent on guaiacol concentration, and the secondary plot of k_{cat} versus guaiacol concentration was linear, with a slope whose gradient gave a value of $(3.5 \pm 0.9) \times 10^4$ $M^{-1} \cdot s^{-1}$ for the second-order rate constant of guaiacol oxidation by an MPO high-oxidation-state compound (results not shown). The specificity for H_2O_2 is defined by the ratio of k_{cat}/K_m and permits a lower limit for the second-order rate constant for the reaction of H_2O_2 with MPO to be calculated. The plot of k_{cat} versus K_m was linear and its slope gave a value of k_{cat}/K_m (as a mean $\pm$ S.D.) of $(6.3 \pm 1.3) \times 10^6$ $M^{-1} \cdot s^{-1}$ (results not shown), in reasonable agreement with the values of 1×10^7 $M^{-1} \cdot s^{-1}$ or 2×10^7 $M^{-1} \cdot s^{-1}$ obtained directly for compound I formation by a transient-state method [31,32].

Table 1 Kinetic parameters for H_2O_2

The k_{cat} and K_m values for H_2O_2 were determined from fitting of the data obtained for guaiacol oxidation by MPO described in Figure 3.

Guaiacol (mM)	k_{cat} (s^{-1})	K_m (μM)
0.2	11 ± 0.2	1.5 ± 0.4
1	38 ± 1	4.4 ± 1.1
5	194 ± 11	34 ± 6
10	325 ± 35	74 ± 25
15	523 ± 57	97 ± 30
20	576 ± 50	83 ± 21
29	770 ± 82	134 ± 47
35	986 ± 76	144 ± 27

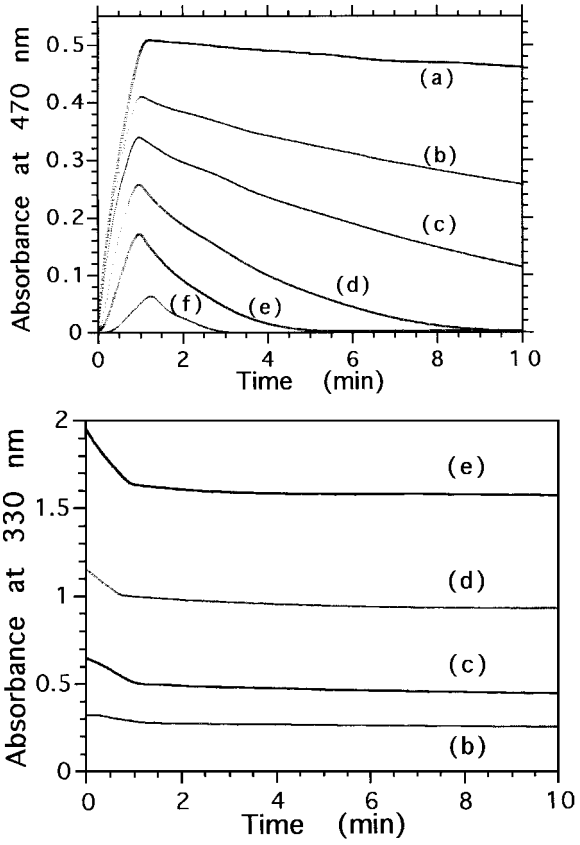

Figure 4 Time course of guaiacol oxidation at various NADPH concentrations (upper panel), and effect of NADPH concentration on its own oxidation time course (lower panel)

Upper panel: incubations contained 1 mM guaiacol, 90 μM H_2O_2, 31 nM MPO and NADPH concentrations, increasing from (a), 0; (b), 50 μM; (c), 100 μM; (d), 200 μM; (e), 300 μM; and (f), 400 μM in 20 mM phosphate buffer, pH 7.0. Reactions were initiated by the addition of MPO. Lower panel: same conditions as in the upper panel were used. Guaiacol concentration was 1 mM and NADPH concentrations were varied as follows (curve labels shown in parentheses): (b), 50 μM; (c), 100 μM; (d), 200 μM; (e), 300 μM.

Oxidation reactions in the presence of reduced pyridine nucleotides

Under steady-state conditions, the formation of BQ was inhibited by NADPH. The kinetics of inhibition were biphasic (Figure 4, upper panel). In the rapid phase, the inhibition was characterized

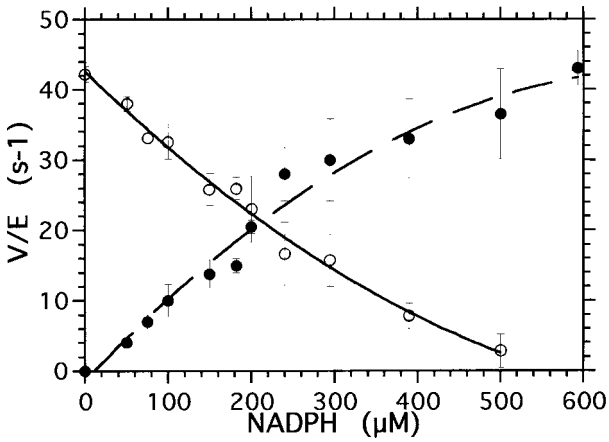

Figure 5 Relative rates of guaiacol and NADPH oxidation in presence of various NADPH concentrations

The rate, V/E, was determined from the initial and/or maximum slope of the time course of guaiacol oxidation measured in the presence of NADPH, 31 nM MPO and 1 mM guaiacol (○). Initial rate, V/E, determined from the linear decrease in A_{330} of NADPH, in the presence of 1 mM guaiacol and 31 nM MPO (●). Data points represent the means of triplicate measurements and the error bars indicate standard deviations.

by a certain lag time, which increased with concentrations of added NADPH, preceding the accumulation of BQ at a steady rate. In the slow phase, the BQ decayed at a rate accelerated slightly by the presence of remaining NADPH.

Under the same steady-state-concentration conditions of H_2O_2, MPO and NADPH, the oxidation of NADPH did not occur over 15 min. This observation confirmed previous reports on the oxidation of NAD(P)H catalysed by the peroxidase/H_2O_2 system, which requires the presence of a mediating molecule at pH 7.0 [18–20,33–35]. Addition of 1 mM guaiacol to the system at $t = 0$ resulted in a dramatic increase in the rate of NADPH oxidation (Figure 4, lower panel). As shown by comparison of corresponding kinetics in Figure 4, synchronized biphasic time courses were detected at the levels of both oxidized guaiacol product and $NADP^+$ formation. Even though the guaiacol concentration was 20-fold higher than that of NADPH, the latter was consumed first, during the lag period detected at the level of guaiacol oxidation. During the time when the transition between the two phases took place, i.e. after 1 min, the amount of oxidized guaiacol reached its maximal level as the rapid $NADP^+$ formation ended. The oxidation of guaiacol and NADPH occurred concurrently. The initial rate and extent of NADPH oxidation both increased with increasing NADPH concentration (Figure 5 and Table 2), whereas those for guaiacol oxidation concomitantly decreased. Whatever concentration of NADPH was used, the two oxidized equivalents of H_2O_2 (90 μM) were almost entirely distributed between the detected oxidized guaiacol and $NADP^+$, as shown by their sum (82 ± 5 μM; n = 12) calculated from the data presented in Table 2. Thus all the added H_2O_2 had been consumed at the end of the rapid phase. In particular, at high NADPH concentrations inhibiting completely guaiacol oxidation, $NADP^+$ formation reached a maximum level equal to the initial H_2O_2 concentration, and its rate of formation tended to become identical with the turnover rate obtained for direct oxidation of guaiacol by MPO in the absence of NADPH (Figure 5 and Table 2). No more $NADP^+$ was produced independently of H_2O_2.

Table 2 Concentrations of oxidized guaiacol and $NADP^+$ at the end of the rapid co-oxidation phase

Results determined from quantitative analyses of the changes in absorbance followed at 470 nm and 330 nm, at the time of 1 min when oxidized guaiacol reached its maximal level and the rapid formation of $NADP^+$ ended, under conditions described in Figure 4. Mean values for three independent experiments are presented.

NADPH (μM)	Oxidized guaiacol (μM)	$NADP^+$ (μM)
0	90 ± 4	0
25	79 ± 3	6 ± 2
50	75 ± 2	11 ± 4
100	57 ± 5	24 ± 6
150	45 ± 7	32 ± 4
200	42 ± 5	40 ± 8
250	33 ± 4	55 ± 9
300	24 ± 4	57 ± 5
385	11 ± 6	64 ± 9
476	7 ± 3	69 ± 4
520	4 ± 2	73 ± 3
593	0	84 ± 5

The initial rate of NADPH oxidation appeared to be saturable with respect to guaiacol, and the apparent second-order rate constant obtained from this curve, k_{cat}/K_m, was $(4.4 \pm 0.2) \times 10^4\ M^{-1} \cdot s^{-1}$; the K_m was 7 ± 1 mM (Figure 6, upper panel, curve b). These values were close to those obtained for the direct steady-state oxidation of guaiacol by MPO (K_m 8.3 ± 1.7 mM) and the value of k_{cat}/K_m of $(5.3 \pm 0.2) \times 10^4\ M^{-1} \cdot s^{-1}$ (Figure 6, upper, curve a). Therefore, provided that the NADPH concentration (500 μM) was capable of inhibiting completely guaiacol oxidation at all concentrations of guaiacol used (below 10 mM), the effects of increasing guaiacol concentration on the stimulation of NADPH oxidation were essentially identical with its effect on its own oxidation rate.

Similarly, the concentration of H_2O_2 had no significantly different effects on the initial oxidation rates of guaiacol and NADPH (Figure 6, lower panel). The initial oxidation rates of guaiacol (Figure 6, lower, curve a) and NADPH (Figure 6, lower, curve b) increased until the concentration of H_2O_2 reached 100 μM. Then a marked inhibition of the rate was clearly shown by a further increase in H_2O_2 concentration. By considering only the non-inhibited part of the plot, Michaelis–Menten analyses yielded values for k_{cat} and K_m of 9 ± 0.3 s^{-1} and 2.5 ± 0.6 μM respectively for H_2O_2 at the level of NADPH (Figure 6, lower, curve b), close to the values determined at the level of guaiacol reported in Table 1.

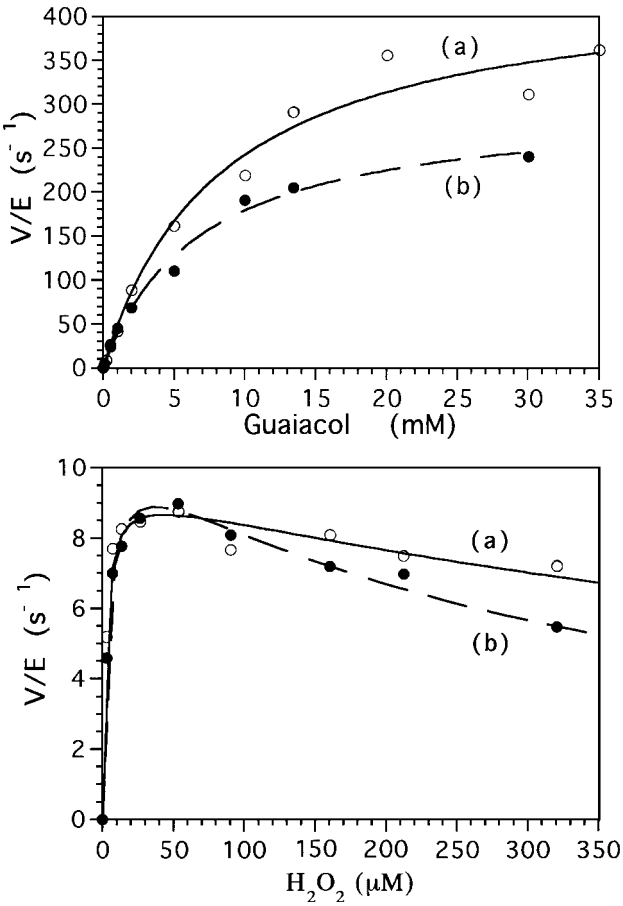

Figure 6 Modulation of the oxidation rate of guaiacol and NADH

Upper panel: effect of guaiacol concentration on guaiacol (curve a) and NADPH (curve b) oxidation rates (*V*/*E*). All reactions were carried out at pH 7.0 using 20 mM phosphate buffer with 23 nM MPO, 90 μM H_2O_2 and varying concentrations of guaiacol in the absence (○) or presence (●) of 500 μM NADPH. Lower panel: effect of H_2O_2 concentration on guaiacol (curve a) and NADPH (curve b) oxidation rates (*V*/*E*). All reactions were carried out at pH 7.0 using 20 mM phosphate buffer with 74 nM MPO, 0.2 mM guaiacol and varying concentrations of H_2O_2 in the absence (○) or presence (●) of 300 μM NADPH. In both panels, the data points represent the means of triplicate measurements and the lines represent fits to the Michaelis–Menten equation.

Mechanistic studies

Redox cycles of guaiacol

To confirm the continuous generation of guaiacol from the reaction of NADPH with the transient oxidized guaiacol, the oxidation of both reductants was studied in the presence of MPO by stepwise addition of H_2O_2 (90 μM aliquots), which allowed us to titrate selectively first NADPH, then guaiacol. Results are illustrated in Figure 7 for an initial NADPH:guaiacol ratio of 2.5. After one cycle of oxidation and reduction, obtained by addition of two aliquots of H_2O_2, no accumulation of oxidized guaiacol appeared as the quantitative oxidation of 180 μM NADPH proceeded. After the second cycle, which led to 70% oxidation of NADPH, oxidized guaiacol reached 50 μM. At the end of the titration of 7–8 aliquots of H_2O_2, i.e. when 630–720 μM H_2O_2 had been added and no more NADPH or guaiacol was oxidized, the amount of oxidized guaiacol formed corresponded to 85% of that of the control experiment performed at the same guaiacol concentration, but in the absence of NADPH (Figure 7, lower panel). An improved yield of 92% was obtained at ratios of NADPH:guaiacol of 0.8 and 1.6, corresponding to a smaller number of cycles of oxidation and reduction. In conclusion, when NADPH oxidation was complete, the final accumulation of oxidized guaiacol was largely unaffected, thereby indicating that guaiacol was hardly consumed at all during this process.

Identification of the oxidized NADPH products

The final product of NADPH oxidation was determined first. When most of the NADPH was oxidized, addition of glucose-6-phosphate and glucose-6-phosphate dehydrogenase induced the formation of NADPH (characterized by a burst in absorbance at 330 nm that accounted for over 95% of the NADPH originally present in the reaction mixture) from the oxidized $NADP^+$ present in solution (Figure 8, upper panel, curve a). This indicated that $NADP^+$ formed by the guaiacol-mediated NADPH oxi-

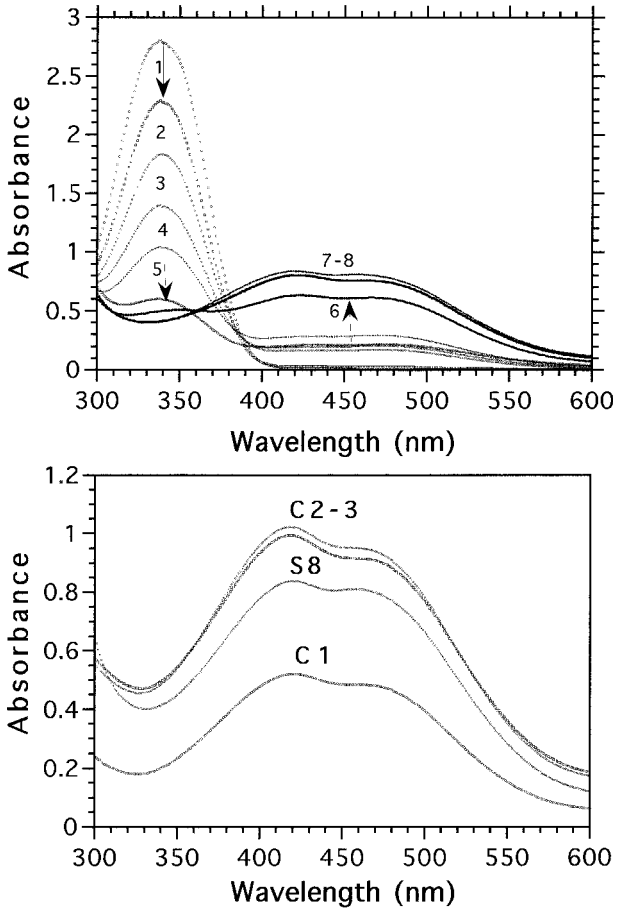

Figure 7 Parallel oxidation of NADPH and guaiacol by H_2O_2 pulses

Upper panel: the reaction was carried out at pH 7.0 using 20 mM phosphate buffer with 125 nM MPO, 200 μM guaiacol, 450 μM NADPH and adding aliquots of 90 μM H_2O_2. Repetitive additions of H_2O_2 were performed approx. every 3–4 min. The values (1–8) correspond to the addition number, and arrows indicate the growth and decay of each peak. Lower panel: a comparison of the spectra of oxidized guaiacol obtained at the end of the titration of eight 90 μM H_2O_2 aliquots in the presence of NADPH (S8) with spectra of oxidized guaiacol obtained in control experiments in the absence of NADPH, after addition of either one (C1) or two or three (C2–3) aliquots of H_2O_2.

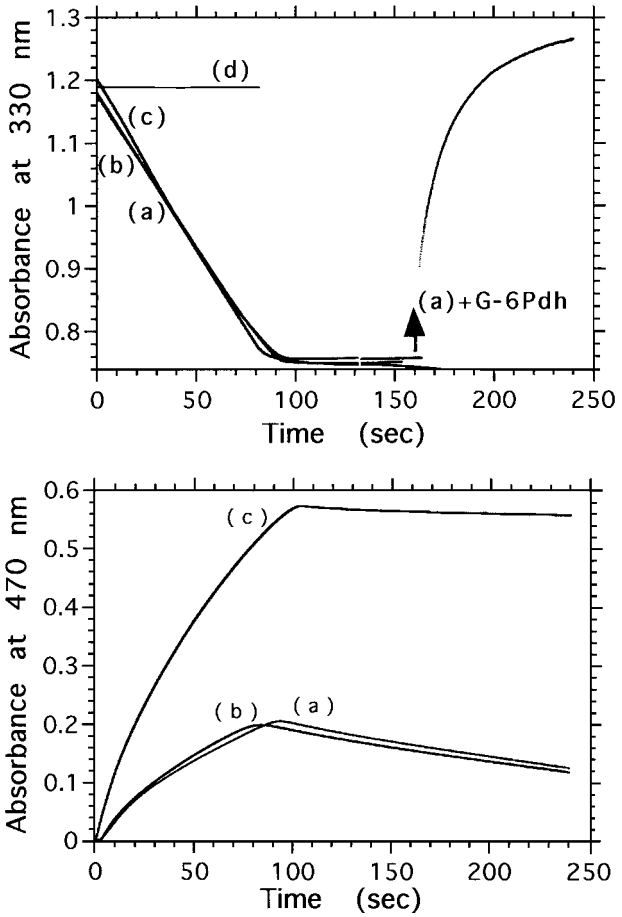

Figure 8 Effect of SOD, anaerobic conditions and catalase on NADPH (upper panel) and guaiacol (lower panel) oxidation time courses

Both assays were performed under the same experimental conditions. Samples contained 200 μM NADPH, 1 mM guaiacol, 110 μM H_2O_2 and 20 nM MPO. Upper panel: NADPH oxidation monitored at 330 nm in the absence (curve a) or presence (curve b) of 1.2 μM SOD; under argon flux (curve c); or in the presence of 0.1 μM catalase (curve d). After 2.5 min of reaction, 5 mM glucose 6-phosphate and 0.1 μM glucose-6-phosphate dehydrogenase (G-6Pdh) were added to recycle $NADP^+$ to NADPH. Lower panel: guaiacol oxidation monitored at 470 nm in the presence of NADPH (curve a); in the presence of NADPH and 1.2 μM SOD (curve b); or in absence of NADPH (curve c).

dation had not been oxidatively degraded any further. Thus the final product of the guaiacol-mediated NADPH oxidation by the MPO/H_2O_2 system is enzymically active $NADP^+$.

Factors controlling the NADPH oxidation mediated by guaiacol metabolites

As expected from previous reports on NAD(P)H co-oxidation [19,20,33–35], $O_2^{-\bullet}$ might be involved in the propagation of NADH oxidation by peroxidases. To further investigate the mechanism of reaction, and the participation of $O_2^{-\bullet}$ in the oxidation of NADPH, we examined the effects of the addition of SOD on the time courses of both guaiacol and NADPH oxidation (Figure 8, upper panel, curves a and b). SOD had no effect in terms of either the rate of modification or the extent of their oxidation. Furthermore, when SOD was added with NADPH at the time when BQ had reached its maximum absorbance level, an absence of modification on its disappearance was observed (results not shown). When the possible role of dioxygen was investigated by repeating the experiments with solutions thoroughly deoxygenated by passing argon through them, there was no observable change in the results (Figure 8, upper, curve c). The absence of any effect suggested that $O_2^{-\bullet}$ did not participate in the NADPH oxidation mediated by transient or final guaiacol oxidation products. It is of interest that the addition of catalase at any time during the reaction inhibited guaiacol and NADPH oxidation (Figure 8, upper, line d), thereby demonstrating a requirement for H_2O_2 in the reaction mixture.

NADPH oxidation mediated by a tyrosine metabolite

Control experiments were performed to determine whether the oxidation mechanism of NADPH might depend on the type of peroxidase (with MPO used here instead of HRP) or, more likely, on the mediating molecule. Correspondingly, studies of the reaction using tyrosine as a catalyst were carried out. Indeed, recently it was established that tyrosine is a substrate for MPO [36], leading to the production of dityrosine by C–C coupling of two transient tyrosyl radicals [37]. Figure 9 shows that NADPH

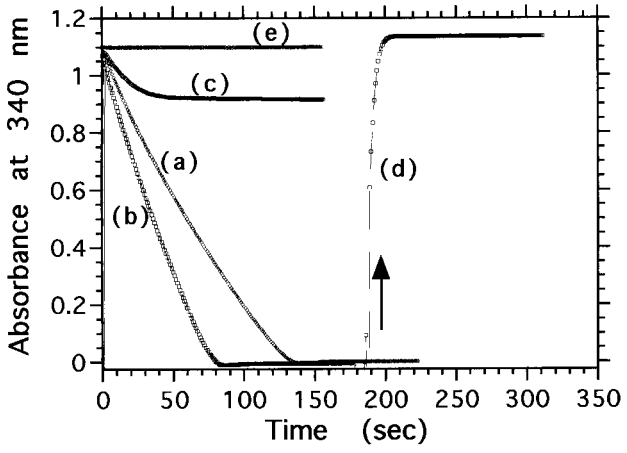

Figure 9 Effect of tyrosine on NADPH oxidation catalysed by MPO

All reactions were carried out at pH 7.0 using 20 mM phosphate buffer with 40 nM MPO, 25 μM H_2O_2, 3 mM tyrosine and 200 μM NADPH, in the absence (curve a) or presence (curve b) of 1μM SOD, or under argon flux (curve c). After 3 min of reaction, 5 mM glucose 6-phosphate and 0.1 μM glucose-6-phosphate dehydrogenase were added to recycle $NADP^+$ to NADPH (curve d). Curve (e) shows the control, without mediator.

oxidation could be obtained in a system containing MPO, H_2O_2 and 3 mM tyrosine. Measurement of the total absorbance variation indicated that 8 mol of NADPH were oxidized by 1 mol of H_2O_2 (Figure 9, curve a). Addition of SOD significantly increased the oxidation rate (Figure 9, curve b). In the absence of dioxygen, the stoichiometry of oxidized NADPH:H_2O_2 became equal to 1 (Figure 9, curve c). Taken together, these data suggest that $O_2^{-\bullet}$ and H_2O_2 are produced in the reaction. The addition of glucose-6-phosphate dehydrogenase to the spent reaction mixture regenerated nearly all of the added NADPH (Figure 9, curve d), confirming that $NADP^+$ was the only oxidized compound produced from NADPH. Similar effects were reported for the co-oxidation of NAD(P)H by the HRP/H_2O_2 system mediated by phenoxyl radicals from thyroxine, various arylamine or phenolic substrates, paracetamol and scopoletin [19,20,34,35].

Reaction of the BQ with NADPH

To clarify the mechanism of guaiacol mediation, and to determine the redox species involved, the reaction of BQ with NADPH was investigated. Study of the oxidation of NADPH was conducted by adding NADPH after the total oxidation yield of BQ had occurred, which corresponded to the complete consumption of H_2O_2 by the enzymic reaction (Figure 1). The results of typical reaction curves, monitored at 330 nm and 470 nm respectively, indicated that NADPH oxidation was synchronized with the disappearance of BQ (results not shown). By consideration of the amplitudes of these curves, the stoichiometry of the reaction corresponded to two disappeared oxidized guaiacol product molecules per molecule of $NADP^+$ formed (2.15 ± 0.25; $n = 8$). This ratio was expected for the reduction of one BQ molecule to biphenol by one NADPH. The decrease in A_{470} due to the reduction of the BQ followed a slow exponential decay curve, and lengthened over 10 min for 300 μM NADPH (Figure 1, curve b), instead of 1 min, as observed above (Figure 4, lower panel). The k_{obs} for guaiacol oxidation product reaction with NADPH was linearly dependent on NADPH concentration, and a second-order rate constant of 16 $M^{-1} \cdot s^{-1}$ was obtained for this reaction (Figure 1, lower panel).

DISCUSSION

Information on guaiacol oxidation by MPO is reported here for the first time. Of interest in this study are the estimates of the rates of guaiacol oxidation and compound I formation for MPO, determined under steady-state conditions. The latter is only 2- to 3-fold lower than the second-order rate constant reported for the direct oxidation of MPO to compound I by H_2O_2 [31,32]; therefore these are in reasonable agreement. It might be useful to compare the rate of guaiacol oxidation by MPO with the reported values for guaiacol oxidation by compound II from other peroxidases. The efficiency of MPO is close to that of TPO [17], but 10-fold lower than that reported for HRP or LPO [17,38]. These differences in rates for various peroxidases could be related to variations in the mechanism and/or the active site. Nevertheless, when considering the reaction of compound II of MPO with various substrates, i.e. the step that is rate-limiting in terms of its turnover, the rate of guaiacol oxidation is close to those rates reported for ascorbic acid [39] and tyrosine [36], substrates known to give rise to transient free radicals [40,41]. Taking into account the relatively slow rate of guaiacol oxidation by MPO, it is tempting to speculate that the presumption that compound II accumulates during the turnover of MPO in the presence of guaiacol might be as valid, as found for other substrates and peroxidases.

We have focused on the mechanism of guaiacol oxidation by the MPO/H_2O_2 system, with characterization of the reactive intermediate products by means of NADPH co-oxidation. It is well established that the oxidation of NAD(P)H by HRP/H_2O_2 under steady-state conditions requires the presence of a mediating molecule that acts as a redox catalyst for NAD(P)H oxidation [18–20,33–35]. In the present paper, several lines of evidence indicate that guaiacol metabolites promote NADPH oxidation in the presence of the MPO/H_2O_2 system; indeed, guaiacol itself stimulated NADPH oxidation. The oxidation of NADPH mediated by either guaiacol or H_2O_2 is described by saturation kinetics close to those established for guaiacol alone. Thus the

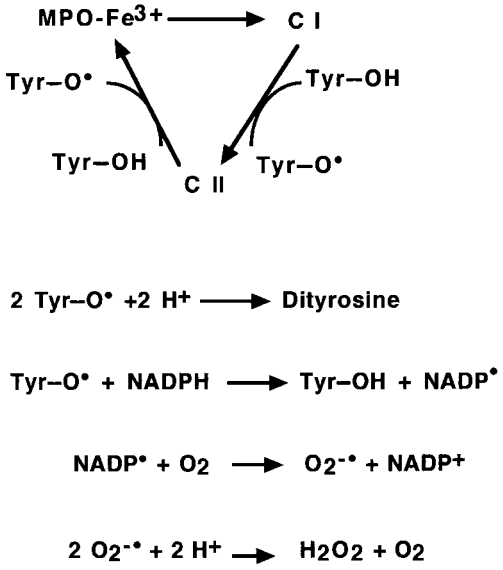

Scheme 1 Proposed mechanism for the tyrosine-mediated indirect oxidation of NADPH by MPO with transient generation of $O_2^{-\bullet}$ and H_2O_2

Abbreviations used: Tyr–OH, tyrosine; Tyr–O•, tyrosyl radical; NADP•, NADP radical; C I and C II, compounds I and II respectively.

NADPH oxidation is totally dependent on the turnover of MPO. In contrast, the presence of NADPH considerably delayed the oxidation of guaiacol by MPO/H_2O_2. However, the decrease in rate cannot be accounted for by competition of NADPH with guaiacol at the active site of MPO. Indeed, guaiacol has no inhibitory effect on NADPH oxidation, as it would be expected to have when two substrates compete for binding at the active site of an enzyme. Finally, the kinetic features support the rationale that the guaiacol oxidation products are responsible for the observed oxidation of NADPH.

Results from redox cycles mediated by H_2O_2 provide further support for multiple cycles of oxidation and reduction carried out by guaiacol acting as an electron carrier, being alternately oxidized/reduced by the MPO/H_2O_2 system and the hydrogen donor respectively. Oxidized guaiacol products were reduced by NADPH as rapidly as they were formed by MPO/H_2O_2, and no BQ accumulated during these reactions, giving the impression of inhibition of guaiacol oxidation.

As expected from previous reports on the phenol-mediated NAD(P)H oxidation by a peroxidase/H_2O_2 system [18–20, 33–35], a free radical mechanism is most frequently involved in the aerobic NAD(P)H oxidation catalysed by the peroxidase/H_2O_2 system. In the present paper, results on tyrosine-stimulated NADPH oxidation, catalysed by MPO, lead to the same conclusion. The MPO/H_2O_2 system catalysed the one-electron oxidation of tyrosine to tyrosyl radical which, in turn, rapidly oxidized NADPH (Scheme 1). Transient tyrosyl radicals are known to oxidize pyridine nucleotides by a direct one-electron transfer process [$k = (6–8) \times 10^7\ M^{-1} \cdot s^{-1}$] [41], which results in the formation of NAD(P)$^{\bullet}$ radical, a potent reductant [$E_{m,7}$ of NAD(P)$^+$/NAD(P)$^{\bullet} = -920$ mV] [42]. Subsequently, the nucleotide radical is capable of rapidly reducing molecular oxygen ($k = 2 \times 10^9\ M^{-1} \cdot s^{-1}$) [43], thus generating $O_2^{-\bullet}$, which dismutates, producing H_2O_2. In this case, both $O_2^{-\bullet}$ and H_2O_2 are generated from the aerobic oxidation of NADPH catalysed by peroxidases. Consequently, a trace amount of H_2O_2 initiates a peroxidase-catalysed aerobic oxidation, and further addition of H_2O_2 is no longer necessary for the reaction to proceed. Thus the stoichiometry of oxidized NADPH:added H_2O_2 is expected to be > 1.

In contrast, results presented here on the guaiacol-mediated NADPH oxidation suggest that a radical did not react with NADPH. This is indicated by the absence of an effect of SOD on the NADPH oxidation rate, showing that the superoxide radical anion is not involved in the NADPH oxidation. Indeed, it is not an oxidase-catalysed reaction, because it does not require dioxygen and can occur in argon. The stoichiometric ratio of the disappearance of NADPH and H_2O_2 was found to be $\leqslant 1$ (Figure 8), while the generation of H_2O_2 in presence of NADPH was observed in tyrosine mediation (Figure 9). Consequently, the comparison of our data on tyrosine- and guaiacol-mediated NADPH oxidation suggests that the stimulated oxidation of NADPH by guaiacol involves a reaction with a two-electron-oxidized metabolite of guaiacol, and not a radical-chain propagation. This conclusion would be consistent with the absence of any report on the determination of the redox potential for the couple G-O$^{\bullet}$/G-OH (where G-OH is the phenolic substrate being reduced and G-O$^{\bullet}$ is the phenoxyl radical), as expected for an unstable or short-lived radical [44].

Among the two-electron-oxidized guaiacol species, either a primary oxidation product, such as the transient guaiacol phenoxyl cation (G-O$^+$), or the final product, the BQ, might be postulated. Our experiments did not support the hypothesis that the final guaiacol oxidation product (BQ) was responsible for the observed oxidation of NADPH. However, BQ is a potent oxidant that can be reduced by a direct two-electron transfer reaction to a biphenol. The data here showed that BQ was most effective in supporting NADPH oxidation, although concurrent measurements at the level of NADPH and BQ allowed the characterization of a slow exchange ($16\ M^{-1} \cdot s^{-1}$) incompatible with the turnover rate of MPO for guaiacol [$k_+ = (4–5) \times 10^4 M^{-1} \cdot s^{-1}$], corresponding to the consumption of one BQ molecule per molecule of oxidized NADPH, as follows:

$$BQ + NADPH \rightarrow BP\text{-}OH + NADP \quad (6)$$

where BP-OH represents biphenol.

Both the timescale and the stoichiometry (2:1, instead of 1:1, for oxidized guaiacol product:NADPH) do not fit the characteristics of NADPH oxidation under steady-state conditions. We therefore conclude that, under steady-state conditions in the presence of MPO/H_2O_2 as described above, NADPH is very likely to be oxidized by an intermediate two-electron oxidation product of guaiacol, hypothesized to be a transient guaiacol phenoxyl cation (G-O$^+$). This species could be generated by the mechanism shown in eqn. (5), i.e, by dismutation of two phenoxyl radicals, which is generally considered to be a faster bimolecular reaction than the coupling reaction between these radicals [eqn. (4)]. It is also very likely that the phenoxyl radical remains tightly bound to the enzyme active site and generates the two-electron-oxidized guaiacol species (G-O$^+$) via a coupling process with compound II [eqn. (3′)]. In the case of such an hypothesis, a direct two-electron transfer could occur between NADPH and G-O$^+$, as follows:

$$NADPH + G\text{-}O^+ \rightarrow NADP^+ + G\text{-}OH \quad (7)$$

We cannot exclude the possibility, at present, of the participation of another type of two-electron-oxidized species; it is hoped that further kinetic and structural investigations will provide an answer to this question.

Differences observed in the mechanism of oxidation of guaiacol catalysed by MPO or TPO (a two-electron mechanism type) and HRP (a one-electron mechanism type) [17] most likely emphasize differences in the active-site environment. The crystal structures of both HRPC and MPO–salicylhydroxamic complex [45,46] revealed a hydrophobic region at the entrance to the distal haem cavity, with three nearby phenylalanines that could accommodate the aromatic substrate-binding site. Results from studies on both MPO and HRP complexes proposed that the first, fast single-electron oxidation of aromatic substrates took place at the haem periphery [46,47]. Indeed, these processes were related to a similar short distance of 0.4 nm between the substrate aromatic ring and the 8-methyl group on the pyrrole ring D [46,48]. In contrast, with respect to the second electron-oxidation step at the level of compound II, the distances from the aromatic-ring carbon atoms to the haem iron were shorter in the MPO–salicylhydroxamic acid complex than the ring-proton-to-haem-iron distances determined for either the HRP or LPO complex [46,48,49]. Indeed, differences exist at the haem level. Besides the existence of a covalently linked haem moiety to the protein in mammalian peroxidases, and not in plant peroxidases [16,50], the reduction potential of the iron is 0.2 V higher in MPO for compound I than in HRP [7,51]. If it is assumed that this redox difference would be maintained at the level of compound II, these characteristics could promote a two-electron type of mechanism for the guaiacol oxidation reaction by MPO.

It is clear from our data that caution must be exercised when using the commonly used guaiacol method for measuring the MPO content in leukocyte or granule extracts [9,10]. NAD(P)H must be eliminated, or at least its concentration diminished, to avoid interference with the assay.

Our results might also have physiological relevance. Provided that the redox potentials of the oxidized compounds produced upon oxidation of substrates by MPO are higher than NADPH, these compounds are likely to act as efficient mediators of NADPH oxidation, and thus may play a regulatory role in controlling NADPH levels. Indeed, NADPH is associated with the activity of NADPH oxidase, involved in the oxidative stress of phagocytes by production of superoxide radical [4]. The production of $O_2^{-\bullet}$ by the cell occurs over a short time, and is abruptly terminated [1,52]. Thus it is conceivable that, as a side reaction, the transient depletion in NADPH resulting from the stimulation of NADPH oxidation by redox mediation may constitute one of the possible causes for termination of the respiratory burst. As a result, the respiratory burst would be expected to be prolonged in the absence of MPO. Consistent with this interpretation, it must be noted that MPO-deficient leucocytes have an increased respiratory burst [53].

In conclusion, the present study provides evidence that guaiacol acts as an electron carrier, being alternately oxidized and reduced by the MPO/H_2O_2 system and NADPH respectively. A two-electron-oxidized species was shown to be essential for this effect, NADPH being directly oxidized to $NADP^+$ without involvement of a transient radical. Finally, co-oxidation is a general property of products generated by peroxidase catalysis; therefore the peroxidase-dependent oxidation of NADPH is a good candidate for providing information about both the transient and final redox states of oxidizing agents generated in the peroxidase–hydroperoxide dependent catalysis. Further studies are currently in progress to validate this assay.

I thank O. Touet and F. Auchère for assisting with preliminary assays. I am indebted to Dr. I. Artaud for fruitful discussions.

REFERENCES

1 Klebanoff, S. J. (1988) in Inflammation: Basic Principles and Clinical Correlates (Gallin, J. I., Golstein, I. M. and Snyderman, R., eds.), pp. 391–444, Raven Press, New York
2 Flohé, L., Beckman, R., Giertz, H. and Loschen, G. (1985) in Oxidative Stress (Sies, H., ed.), pp. 403–435, Academic Press, New York
3 Rossi, F., Romeo, D. and Patriarca, P. (1972) J. Reticuloendothel. Soc. **12**, 127–149
4 Morel, F., Doussière, J. and Vignais, P. V. (1991) Eur. J. Biochem. **201**, 523–546
5 Winterbourn, C. C. (1990) in Oxygen Radicals: Systemic Events and Disease Processes (Das, D. K. and Essman, W. B., eds.), pp. 31–70, Karger, Basel
6 Thomas, E. L. and Learn, D. B. (1991) Peroxidases Chem. Biol. **1**, 83–104
7 Hurst, J. K. (1991) Peroxidases Chem. Biol. **1**, 37–62
8 Yamazaki, I. (1977) in Free Radicals In Biology (Pryor, W. A., ed.), **3**, pp. 183–218, Academic Press, New York
9 Chance, B. and Maehly, A. C. (1964) Methods Enzymol. **2**, 764–775
10 Klebanoff, S., Waltersdorph, A. M. and Rosen, H. (1984) Methods Enzymol. **105**, 399–403
11 Lindgren, B. O. (1960) Acta Chem. Scand. **14**, 2089–2096
12 Booth, H. and Saunders, B. C. (1956) J. Chem. Soc. 940–948
13 Harauchi, T. and Yoshizaki, T. (1982) Anal. Biochem. **126**, 278–284
14 Bertrand, G. (1904) Ann. Inst. Pasteur **18**, 116–120
15 Doerge, D. R., Divi, R. L. and Churchwell, M. I. (1997) Anal. Biochem. **250**, 10–17
16 Dunford, H. B. (1991) Peroxidases Chem. Biol., **2**, 1–24
17 Nakamura, M., Yamazaki, I., Kotani, T. and Ohtaki, S. (1985) J. Biol. Chem. **260**, 13546–13552
18 Klebanoff, S. J. (1962) Biochim. Biophys. Acta **56**, 460–469
19 Takayama, T. and Nakano, M. (1977) Biochemistry **16**, 1921–1926
20 Subrahmanyam, V. V. and O'Brien, P. J. (1985) Chem. Biol. Interact. **56**, 185–199
21 Capeillere-Blandin, C. (1994) in Metals Ions In Biological Systems: Eurobic II 1994 (Bertini, I. ed.), pp. 72
22 Capeillere-Blandin, C., Masson, A. and Descamps-Latscha, B. (1991) Biochim. Biophys. Acta **1094**, 55–65
23 Suzuki, K., Yamada, M., Akashi, K. and Fujikura, T. (1986) Arch. Biochem. Biophys. **245**, 167–173
24 Svensson, B. E., Domeij, K., Lindvall, S. and Rydell, G. (1987) Biochem. J. **242**, 673–680
25 Beers, Jr., R. F. and Sizer, I. W. (1952) J. Biol. Chem. **195**, 133–140
26 Casella, L., Poli, S., Gullotti, M., Selvaggini, C., Beringhelli, T. and Marchesini, A. (1994) Biochemistry **33**, 6377–6386
27 Newsmeyer, S. and Ortiz de Montellano, P. R. (1995) J. Biol. Chem. **270**, 19430–19438
28 Bakkenist, A. R. J., Wever, R., Vulsma, T., Plat, H. and Van Gelder, B. F. (1978) Biochim. Biophys. Acta **524**, 45–54
29 Hoogland, H., Dekker, H. L., van Riel, C., van Kuilenburg, A., Muijers, A. O. and Wever, R. (1988) Biochim. Biophys. Acta **955**, 337–345
30 Kettle, A. J. and Winterbourn, C. C. (1988) Biochem. J. **252**, 529–536
31 Bolscher, B. G. and Wever, R. (1984) Biochim. Biophys. Acta **788**, 1–10
32 Marquez, L. A., Huang, J. T. and Dunford, H. B. (1994) Biochemistry **33**, 1447–1454
33 Michot, J. L., Virion, A., Deme, D., De Prailaune, S. and Pommier, J. (1985) Eur. J. Biochem. **148**, 441–445
34 Keller, R. J. and Hinson, J. A. (1991) Drug Metab. Dispos. **19**, 184–187
35 Marquez, L. A. and Dunford, H. B. (1995) Eur. J. Biochem. **233**, 364–371
36 Marquez, L. A. and Dunford, H. B. (1995) J. Biol. Chem. **270**, 30434–30440
37 Gross, A. J. and Sizer, I. W. (1959) J. Biol. Chem. **234**, 1611–1614
38 Yamazaki, I. and Yokota, K. (1973) Mol. Cell. Biochem. **2**, 39–52
39 Marquez, L. A., Dunford, H. B. and Van Wart, H. (1990) J. Biol. Chem. **265**, 5666–5670
40 Yamazaki, I., Mason, H. S. and Piette, L. (1960) J. Biol. Chem. **235**, 2444–2449
41 Forni, L. G. and Willson, R. L. (1986) Biochem. J. **240**, 897–903
42 Farrington, J. A., Land, E. J. and Swallow, A. J. (1980) Biochim. Biophys. Acta **590**, 273–276
43 Land, E. J. and Swallow, A. J. (1971) Biochim. Biophys. Acta **234**, 34–42
44 Wardman, P. (1989) Phys. Chem. Ref. Data **18**, 1637–1755
45 Gajhede, M., Schuller, D. J., Henriksen, A., Smith, A. T. and Poulos, T. L. (1997) Nat. Struct. Biol. **4**, 1032–1038
46 Davey, C. A. and Fenna, R. E. (1996) Biochemistry **35**, 10967–10973
47 Ator, M. A. and Ortiz de Montellano, P. R. (1987) J. Biol. Chem. **262**, 1542–1551
48 Sakurada, J., Takahashi, S. and Hosoya, T. (1986) J. Biol. Chem. **261**, 9657–9662
49 Modi, S., Digambar, V. and Mitra, S. (1989) Biochim. Biophys. Acta **996**, 214–225
50 Fenna, R. E., Zeng, J. and Davey, C. (1995) Arch. Biochem. Biophys. **316**, 653–656
51 Hayashi, Y. and Yamazaki, I. (1979) J. Biol. Chem. **254**, 9101–9106
52 Edwards, S. W. and Swan, T. F. (1986) Biochem. J. **237**, 601–604
53 Stendhal, O., Coble, B., Dalhgren, C., Hed, J. and Molin, L. (1984) J. Clin. Invest. **73**, 366–373

Received 8 July 1998/3 September 1998; accepted 1 October 1998